Comparative RNA-sequencing analysis of the prostate in a mouse model of benign prostatic hyperplasia with bladder outlet obstruction

Xiaohu Tang[1,2] · Zhiyan Liu[3] · Jingwen Ren[3] · Ying Cao[1] · Shujie Xia[4] · Zhaolin Sun[1] · Guangheng Luo[2]

Abstract

In ageing men, benign prostatic hyperplasia (BPH) is a chronic disease that leads to progressive lower urinary tract symptoms (LUTS) caused by obstruction of the bladder outlet (BOO). Patients with LUTS (such as increased frequency and urgency of urination) and complications of BOO (such as hydronephrosis and bladder stones) are at risk of serious health problems. BPH causes a rapidly rising burden of LUTS far exceeding that of other urological conditions. Treatment outcomes are unsatisfactory for BPH largely due to the lacking of fully understanding of the pathogenesis. Hormonal imbalances related to androgen and oestrogen can cause BPH, but the exact mechanism is still unknown, even the animal model is not fully understood. Additionally, there are no large-scale data to explain this mechanism. A BPH mouse model was established using mixed slow-release pellets of testosterone (T) and estradiol (E2), and we measured gene expression in mouse prostate tissue using RNA-seq, verified the results using qRT−PCR, and used bioinformatics methods to analyse the differentially expressed genes (DEGs).

Keywords RNA-seq · BPH · BOO · Testosterone · Estradiol

Introduction

Benign prostatic hyperplasia (BPH) is one of the most common diseases in older men, and it affects more than half of all men over the age of 50 years [1]. Its incidence increases further with age, reaching up to 80% in 80-year-old men [2]. Compression of the urethra by an enlarged prostate is the main factor involved in the progression of BPH; this enlargement is characterized by an increase in the number and size of prostate epithelial and stromal cells in the periurethral region [3]. Progressive enlargement of the prostate can lead to compression of the urethra and lead to bladder outlet obstruction (BOO), which can manifest as LUTS [4]. This condition seriously affects the quality of life of patients. BPH is the highest health burden among conditions of the urological system [5]. Although there are many ways to treat BPH, such as alpha1-blockers [6], 5α-reductase inhibitors (5-ARI) [7], and transurethral resection of the prostate (TURP)[8], ejaculation disorders, loss of sexual desire [9], and lower blood pressure [10] can occur with current treatment options [9]; most minimally invasive treatments also destroy the urethra or the prostate, while removing the prostate increases the occurrence of post-operation urinary tract infection [11], affecting sexual function [12] and causing other effects. Additionally, current treatment does not control disease progression in all patients [13, 14].

The pathogenesis of BPH is complex and may be related to the balance in cell proliferation and apoptosis [15], the androgen receptor [16], epithelial mesenchymal transformation [17] and estrogen and androgen imbalance [18], and the molecular mechanisms underlying the clinical phenotype have not yet been fully revealed [19]. Hormonal imbalance related to estrogen and androgen may be one of the important factors causing BPH [20]. As the target organ of sex hormones, androgen and estrogen both regulate the growth of the prostate. It is well known that the prostate is

✉ Guangheng Luo
luoguangheng1975@126.com

1   Medical College, Guizhou University, Guiyang 550025, Guizhou, China

2   Department of Urology Surgery, Guizhou Province People's Hospital, Guiyang 550002, China

3   Guizhou Medical University, GuiyangGuizhou 550025, China

4   Department of Urology Surgery, Shanghai First People's Hospital, Shanghai Jiao Tong University, Shanghai 201620, China

an androgen-dependent organ, but interestingly, testosterone levels reach their peak during early adulthood in men and gradually decrease (1–2% per year)[21], and estrogen levels remain unchanged or slightly decreased, which leads to an increase in the ratio of estrogen to androgen, which can induce the proliferation of stromal cells and their expression of inflammatory factors in individuals with BPH [22]. The estrogen receptor and G protein-coupled estrogen receptor accelerate the progression of BPH by inducing prostatic fibrosis [23]. The coinduction of androgen and estrogen signalling has been shown to accelerate prostatic hyperplasia in dogs and lead to bladder outlet obstruction [24], but the specific mechanism through which estrogen and androgen imbalance affect BPH is still unclear. For a potential breakthrough in BPH treatment, comprehensive research is needed to enable an understanding of the relevant molecular mechanism of BPH development. The existing BPH models rarely have physiological hormone levels associated with the progression of human benign prostatic hyperplasia so it is necessary to establish a mouse model of BPH combined with BOO based on the principle of estrogen and androgen imbalance to further study the pathogenesis of BPH. In addition to 5α-reductase, estrogen and androgen, and their receptor-related genes, BPH is associated with the elevated expression of many genes, which mainly include growth factors; BPH has been found to be associated with abnormal expression of growth factors such as FGF [25], TGF-β [26], EGF [27], and IGF [28]. For example, bFGF can promote the proliferation of prostate fibroblasts cultured in vitro, and prostate stromal cells with high expression of bFGF can stimulate the proliferation of prostate epithelial cells in a paracrine manner [29, 30]. In addition, it was found that the abnormal expression of other genes can promote prostatic hyperplasia; for example, the COX-2/PGE signalling pathway is involved in the progression of BPH [31]. However, the molecular mechanism through which oestrogen and androgen imbalance promotes BPH is not fully understood. RNA-sequencing (RNA-seq) has been widely used in medicine, biology, and other fields [32, 33]; for instance, Magdalena Derbis et al. [34] conducted RNA-seq analyses of the striatum to gain insight into the molecular changes caused by ASO-CCG treatment. Milanez-Almeida et al. [35] recently showed that gene expression data obtained using RNA-seq from The Cancer Genome Atlas (TCGA) could be used to predict survival or the progression-free interval better than classic clinical prognostic factors, such as age at diagnosis, sex, and tumour stage. Therefore, RNA-seq is a key tool for studying disease and biology [36], and it may be beneficial for discovering novel therapeutic targets [37].

Therefore, in this study, a mouse model of BPH combined with BOO was established using testosterone (T) and estradiol (E2) slow-release pellets, and RNA-seq was used to evaluate transcriptomic changes in BPH mice. The reliability of the BPH mouse model was also evaluated by analyses of gross specimens, pathology, and RNA expression, and finally, the key genes, pathways, and infiltrating immune cells were revealed by bioinformatics analysis. In conclusion, the results of this study provide a reference for identifying the potential targets of BPH for treatment.

Materials and methods

Environmental conditions and establishment of animal model

A total of twenty-two 6- to 8-week-old male C57BL/6 mice (Chongqing TengXing Biotechnology Co. Ltd, China) with an average weight of approximately 20 g were used. The animal housing was maintained at 20–25 °C and 40~75% relative humidity. Indoor lighting consisted of 12 h of light and darkness (split between 8 am and 8 pm), and the animals had free access to food and water. All procedures involving animals were approved by the Ethics Committee of Guizhou Provincial People's Hospital (Ethics approval No. 2022–020). After 1 week of acclimatization, twenty-two mice were randomly divided into two groups (control group: Con group; T + E2 slow-release pellet group: T + E2 group) of eleven mice each; eight mice from each group were used for observation data statistics and prostate pathological examination, and the remaining three mice were used only for RNA-seq. With the aid of a pellet press (Parr Instrument Company, USA), T + E2 was made into a cylindrical solid pill with a diameter of approximately 2 mm and a length of approximately 3 mm, with a total weight of approximately 28.6 mg (T: E2 = 10: 1). After preparing the skin on the back of the mouse, subcutaneous local anaesthesia was performed with 1% lidocaine, and one pill was placed in the incision (Fig. 1A), while the control group received only a dorsal skin incision and suture without the treatment. In the T + E2 group, the pellet in each mouse was replaced with 1 new slow-release pellet each month, and the control group underwent the same operation as described previously.

Tissue samples

After 12 weeks, the mice were killed with carbon dioxide; the bladder was examined for stones using a cystoscope as we described before [38]; and their urethra, bladder, prostate, kidney, and testis were immediately obtained. The length of the urethra in the prostate was measured using an accurate calliper, and the volume of the bladder when it was full was estimated by measuring the length of the diameter of the bladder and weighing the prostate.
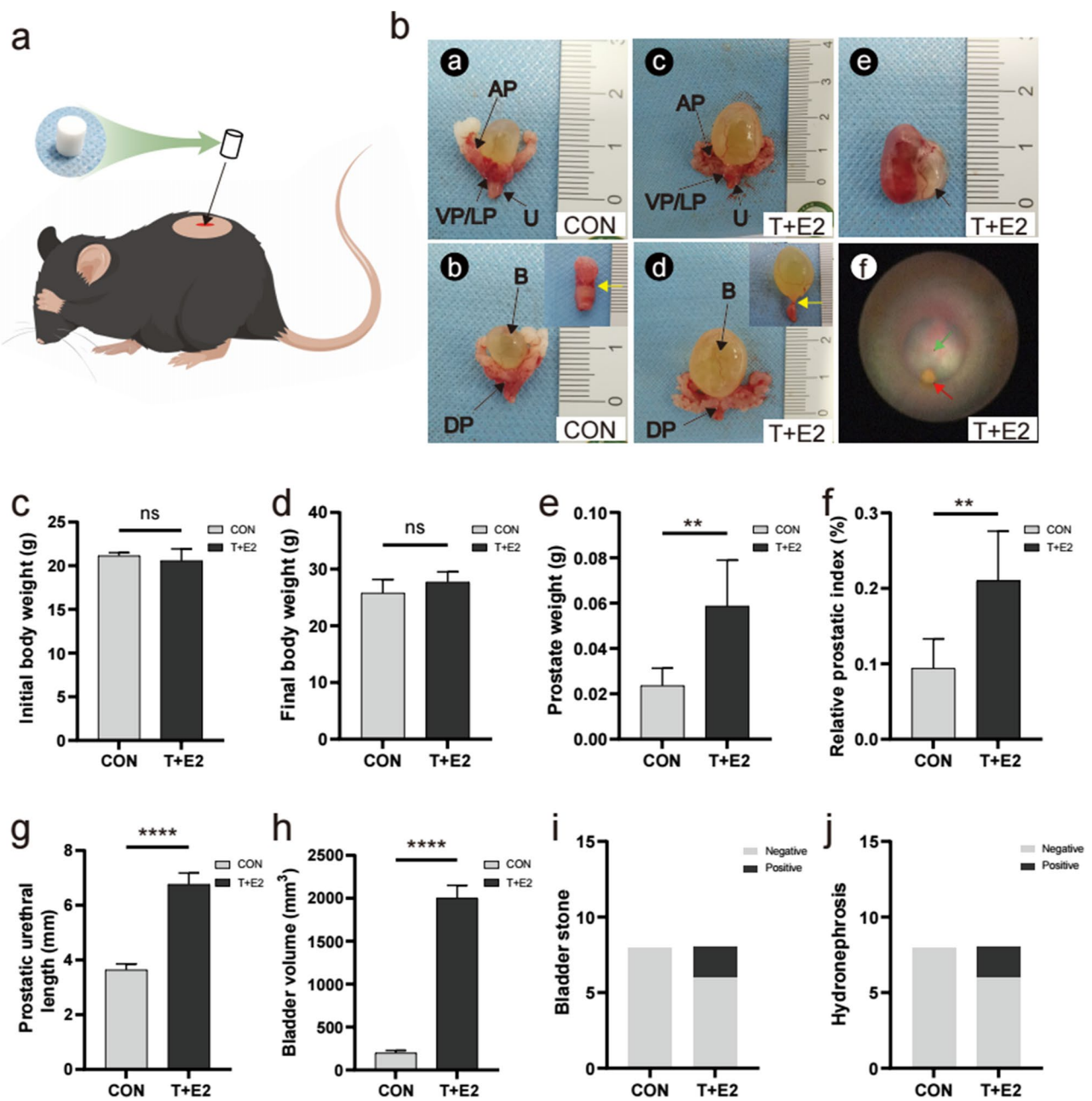
Fig. 1 Effects of T and E2 treatment on the gross and urogenital pathology of mice. **A** Mice were implanted subcutaneously with T+E2 slow-release pellets: **B** (1) Ventral view of the prostate and urethra of the CON group; (2) dorsal view of the prostate and bladder of the CON group (the yellow arrowhead indicates the connecting site of the urethra and bladder in the subplot); (3) ventral view of the prostate and urethra of the T+E2 group; (4) dorsal view of the prostate and bladder of the T+E2 group (the yellow arrowhead indicates the connecting site of the urethra and bladder in the subplot); (5) hydronephrosis of the T+E2 group (arrow marks the renal pelvis); (6) endoscopic observation of a stone in the bladder (red arrowhead), and green arrow indicates bladder lumen; **C** initial body weight; **D** final body weight; **E** prostate weight; **F** relative prostatic index: "Prostate weight"/ "Final body weight"×100%; **G** prostatic urethral length; **H** bladder volume (Formula: volume = Length x width x height x (π/6)); **I** discovery of bladder stones; **J** discovery of hydronephrosis. AP = anterior prostate, VP/LP = ventral prostate/lateral prostate, U = urethra, DP = dorsal prostate, B = bladder. *$P < 0.05$; **$P < 0.01$; ***$P < 0.001$; ****$P < 0.0001$; ns, not significant

Haematoxylin–Eosin (HE)

The fixed tissue embedded in paraffin was sectioned into 5-μm-thick sections. After dewaxing and rehydration, sections were stained with haematoxylin and eosin (H&E) according to standard procedures for light microscopic observation. The prostate epithelial thickness, cross-sectional area of the urethral lumen, renal parenchymal thickness, and detrusor muscle thickness of the bladder were measured and analysed by ImageJ software (National Institutes of Health, USA).

High-throughput RNA-Seq

The total RNA isolated from the prostate tissues ($n = 3$ for each group) was used as input material to prepare RNA samples. Sequencing libraries were generated using the Illumina TruSegTM RNA Sample Preparation Kit (Illumina) following the manufacturer's instructions. The libraries were sequenced on an Illumina HiSeg X-ten System according to the manufacturer's instructions (Shanghai Biotechnology Co.).

Differentially expressed gene (DEG) analysis

DEG analysis was performed by the R package "DESeq2" for the identification of DEGs using the cut-off criteria of |log2 Fc| > 1 and an adjusted P value of < 0.05. Principal component analysis (PCA) plots were generated by the "ggplot2" package in R. PCA and intersample correlation were carried out by the "DESeq2" package in R (version 4.1.3). Correlation heatmap, volcano, and pheatmap plots were plotted in R using the "ggplot2" package and "ComplexHeatmap" package.

Gene ontology (GO) and kyoto encyclopedia of genes and genomes (KEGG) functional enrichment analysis

The Metascape website (http://metascape.org/gp/index.html#/main/step1) is an effective and efficient portal designed for experimentalists [39]. To elucidate the biological functions of the DEGs, pathway enrichment analysis was performed using KEGG signalling and GO analyses. Metascape was also used to calculate the enrichment terms for up- and downregulated DEGs separately. The top 20 clusters of enriched terms (GO/KEGG terms) are each visualized using a heatmap format, which are coloured based on P values.

Protein−Protein interaction (PPI) network analysis of DEGs and correlation analyses

Using default parameters, Metascape was used to generate a PPI network with molecular complex detection (MCODE)

components, and Cytoscape software (Version 3.9.1) was used for further analysis. We first calculated the top 30 hub genes calculated by each algorithm (betweenness, Bottle-Neck, degree, radiality, stress) of the cytoHubba plugin in Cytoscape and then screened for genes that were shared with the MCODE seed genes. We continued to explore the relevance of these key genes in normal and hyperplastic prostate tissue (Spearman approach) using the Genotype-Tissue Expression (GTEx) and Gene Expression Omnibus (GEO) databases. GTEx data were obtained from UCSC Xena (https://xenabrowser.net/) and visualized by the package "ggplot2" in R. We downloaded transcriptomic data for all BPH patients from GSE101486, GSE104749, GSE119195, GSE28204, and GSE5377 in GEO. The expression levels obtained from the 5 GEO datasets were normalized using the R package 'sva', and the data were visualized using the R package "ggplot2". Then, we used the genemania plugin in Cytoscape to explore the association between the key genes.

Gene set enrichment analysis (GSEA) and gene set variation analysis (GSVA)

GSEA is a computational method that determines whether an a priori defined set of genes shows statistically significant, concordant differences between two biological states [40], and the GO/KEGG annotations for GSEA were performed and visualized with the "clusterprofiler" package in R. GSVA, a nonparametric, unsupervised method for estimating gene set enrichment variations in gene expression data, was used to analyse gene set enrichment variations [41]. Then, GO and KEGG results were analysed by the "GSVA" package and visualized by the "ggplot2" R package.

Generation of the ceRNA network

According to the ceRNA hypothesis, lncRNAs (circRNAs) act as molecular sponges that compete with mRNAs for binding to miRNAs, thus inhibiting their activity [42]. The ceRNA network is widely documented as a posttranscriptional regulatory network that participates in many biological processes. We selected the modules of interest in the PPI network to identify ceRNAs and predicted and visualized the interactions of DEmRNAs-miRNAs and miRNAs-lncRNAs (CircRNA) by StarBase (https://starbase.sysu.edu.cn/) and Cytoscape (Version 3.9.1).

Assessment of immune infiltration

To explore the immune microenvironment, we performed CIBERSORT analyses to estimate how many infiltrating immune components were present in the samples [43]. We first obtained the mouse immune cell dataset [44], and the "CIBERSORT" package in R software was used

to investigate possible associations between the genes and immune cells to predict the relative proportions of 25 infiltrating immune cell subtypes, with a total of 1000 permutations performed.

Quantitative real-time RT−PCR

TRIzol (Takara) was used to extract total mRNA, and the PrimerScriptTM RT Reagent Kit (Takara) was used to synthesize cDNA. A SYBR Green PCR kit (Takara Biotechnology Co., Ltd.) was used for qRT−PCR performed using the CFX96 Touch qRT−PCR System (Bio-Rad). PCR data were analysed using the $2 - \Delta\Delta Cq$ method and are expressed as the fold change relative to GAPDH expression levels. All experiments were repeated three times. All primers are listed in Table S1.

Statistical analysis

GraphPad Prism software (version 9.3.0 for Windows) and R software (version 4.1.3) were used to perform the statistical analyses and data visualization. Wilcoxon tests or Student's unpaired t tests were used to compare data. The correlation analysis was performed by Spearman correlation. Differences were considered significant when $P < 0.05$ (*$P < 0.05$; **$P < 0.01$; ***$P < 0.001$; ****$P < 0.0001$; ns = not significant, $P > 0.05$).

Results

T + E2 treatment induction of BPH and BOO in mice

After 12 weeks of treatment with T + E2 slow-release pellets, all mice survived with good mental status, normal diet and activity, and no hormone-related adverse effects, such as hair loss, but there was a slightly hunched posture during urination in the T + E2 group. The volume of the prostate glands in the T + E2 group was uniformly larger than that in the control group (CON group; Fig. 1B, 2), and bladder volume was significantly higher when the bladder was full (Fig. 1B, 3, 4); the urethra, which was covered by the prostate gland, was narrowed so that more pressure was required to pass the urine from the bladder through the urethra in the T + E2 group (Fig. 1B, 2, 4). Two mice in the T + E2 group suffered from unilateral hydronephrosis (Fig. 1B, 5). More interestingly, we found small stones in the bladder in the T + E2 group, while this phenomenon did not occur in the CON group (Fig. 1B, 6). There were no significant differences in body weights (initial and final body weights) between the CON and T + E2 groups ($P > 0.05$, Fig. 1C–D). The weight of the prostate in the T + E2 group was significantly higher than

that in the CON group (+ 148.16%, $P < 0.01$, Fig. 1E), and similarly, the relative prostate index in the T + E2 group also increased (+ 184.22%, $P < 0.01$, Fig. 1F). The urethral length of the prostatic portion in the mice in the T + E2 group was increased (+ 85.90%, $P < 0.0001$, Fig. 1G). The volume of the bladder upon filling was significantly higher in the T + E2 group (+ 905.02%, $P < 0.0001$, Fig. 1H), and two mice with bladder stones and hydronephrosis were found in the T + E2 group (Fig. 1I–J).

T + E2 treatment causes BPH pathological features

After 12 weeks of treatment with T + E2 slow-release pellets, the epithelial cells of the prostate gland in mice had significantly proliferated, the cytoplasm was full, there were epithelial nodules and an accumulation of epithelial cells, and the lumen of the prostatic ducts was also relatively smaller (Fig. 2A). The epithelial thickness of the prostate gland in the T + E2 group was significantly greater than that in the CON group (+ 369.71%, $P < 0.0001$, Fig. 2B). The urethral opening was relatively narrower in the T + E2 group than in the CON group, with signs of extraluminal compression of the urethral lumen (Fig. 2C) and a reduction in urethral cross-sectional area of approximately 73.83% ($P < 0.01$, Fig. 2D). The parenchymal thickness of the hydronephrotic kidney in the T + E2 group tended to lower than that in the CON group (Fig. 2E). In the T + E2 group, the bladder detrusor was significantly thinner (Fig. 2F) than that in the CON group, with a reduction in thickness of approximately 50.83% ($P < 0.0001$, Fig. 2G).

DEG analysis and verification

Overall, there were 833 mRNAs with significantly different expression between the T + E2 group and the CON group (Table S2), including 523 upregulated (Table S3) and 310 downregulated mRNAs (Table S4). Hierarchical clustering heatmaps (Fig. 3A) and volcano plots (Fig. 3B) show the differences in gene expression between the two groups. In PCA clustering analysis, samples obtained within the same group were more tightly clustered, and there were significant expression differences between the two groups (Fig. 3C). Samples from the same group were strongly correlated with each other, with significant differences between different groups (Fig. S1). To further validate the sequencing results, the levels of 6 randomly selected mRNAs were measured using qRT−PCR, and the difference between the two groups was significant ($P < 0.05$) and followed the same trend as the sequencing results, suggesting accurate and reliable sequencing results.
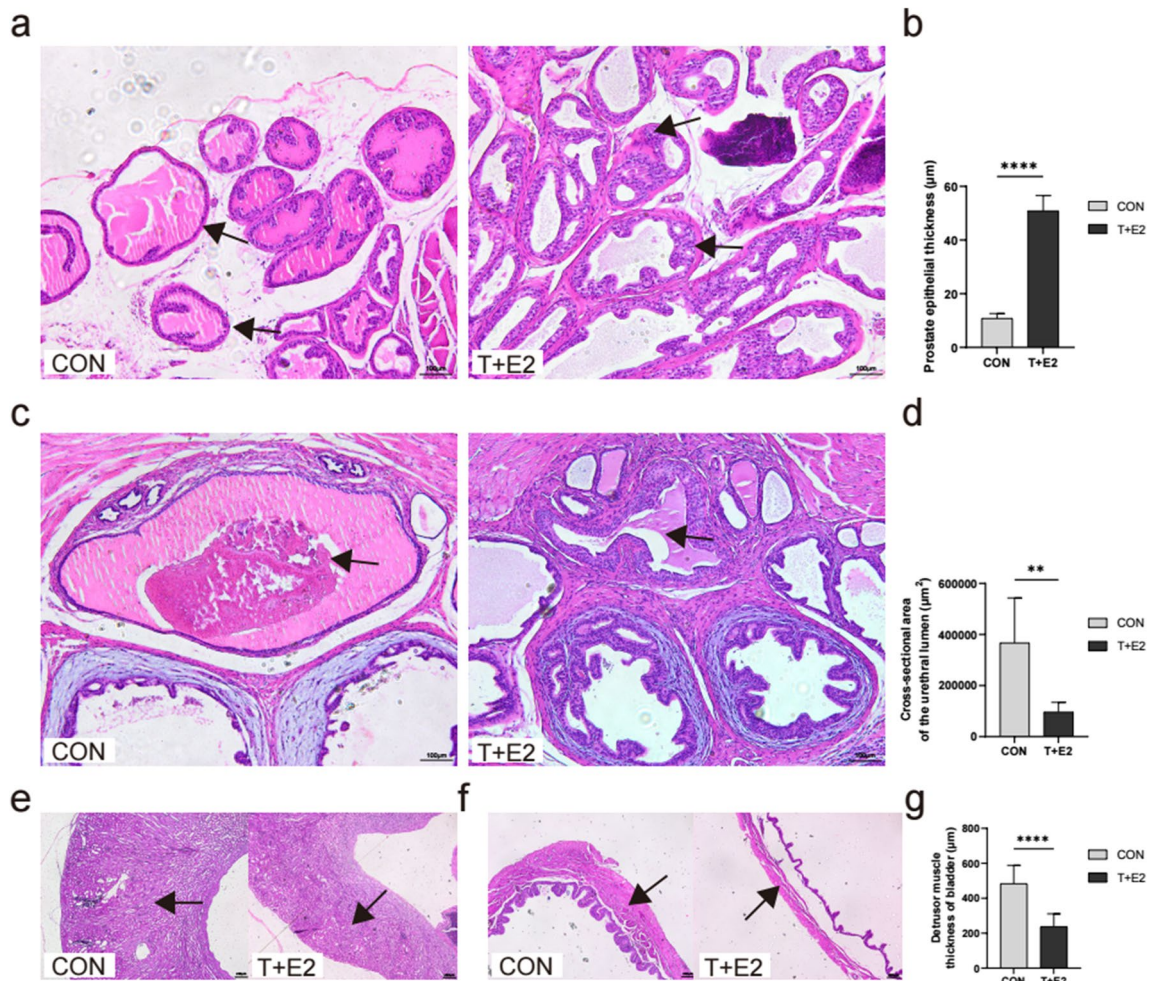
Fig. 2 Pathological examination of prostate in mice. **A** Comparisons of HE staining images of prostate tissues between CON and T+E2 group (arrow head: prostate epithelial cells; scale bar=100 μm); **B** compared with CON group, the thickness of prostate epithelial cells in T+E2 group increased significantly; **C** comparison of the urethral lumen in prostate between the CON and T+E2 groups (arrow head: urethral lumen; scale bar=100 μm); **D** compared with CON group, the cross-sectional area of the urethral cavity in T+E2 group was significantly reduced; **E** comparison of renal parenchymal thickness between the CON and T+E2 groups (arrow head: renal parenchyma; scale bar=200 μm); **F** comparison of bladder detrusor between the CON and T+E2 groups (arrow head: bladder detrusor; scale bar=200 μm); **G** compared with CON group, the detrusor muscle of bladder in T+E2 group was significantly thinner. *$P<0.05$; **$P<0.01$; ***$P<0.001$; ****$P<0.0001$; ns, not significant

Functional annotation and pathway enrichment analysis

GO analysis showed that the DEGs were mainly enriched in modified amino acid binding, import into the cell, cellular-modified amino acid metabolic process, ion homeostasis, and amide transport (Fig. 4A, Table S5). Enrichment analysis of the upregulated and downregulated genes revealed that the upregulated DEGs were mainly enriched in the production of molecular mediator of immune response, endopeptidase inhibitor activity, and oxidoreductase activity, while the downregulated DEGs were mainly enriched in cation transmembrane transporter activity, thyroid hormone transport, and neuronal cell body. Up- and downregulated

genes were mainly coenriched in ion homeostasis, amide transport, modified amino acid binding, regulation of hormone levels, and cellular modified amino acid metabolic process (Fig. 4B, Table S6).

The results of KEGG enrichment analysis showed that the DEGs were mostly enriched in transport of small molecules, mineral absorption, amino acid metabolism, oxidative stress, redox pathway, prostaglandin synthesis, and regulation (Fig. 4C, Table S7). KEGG enrichment analysis of the up- and downregulated DEGs also revealed that the upregulated DEGs were mainly enriched in the regulation of insulin-like growth factor (IGF) transport and uptake by insulin-like growth factor binding proteins (IGFBPs), passive transport by aquaporins, and other glycan degradation, while the
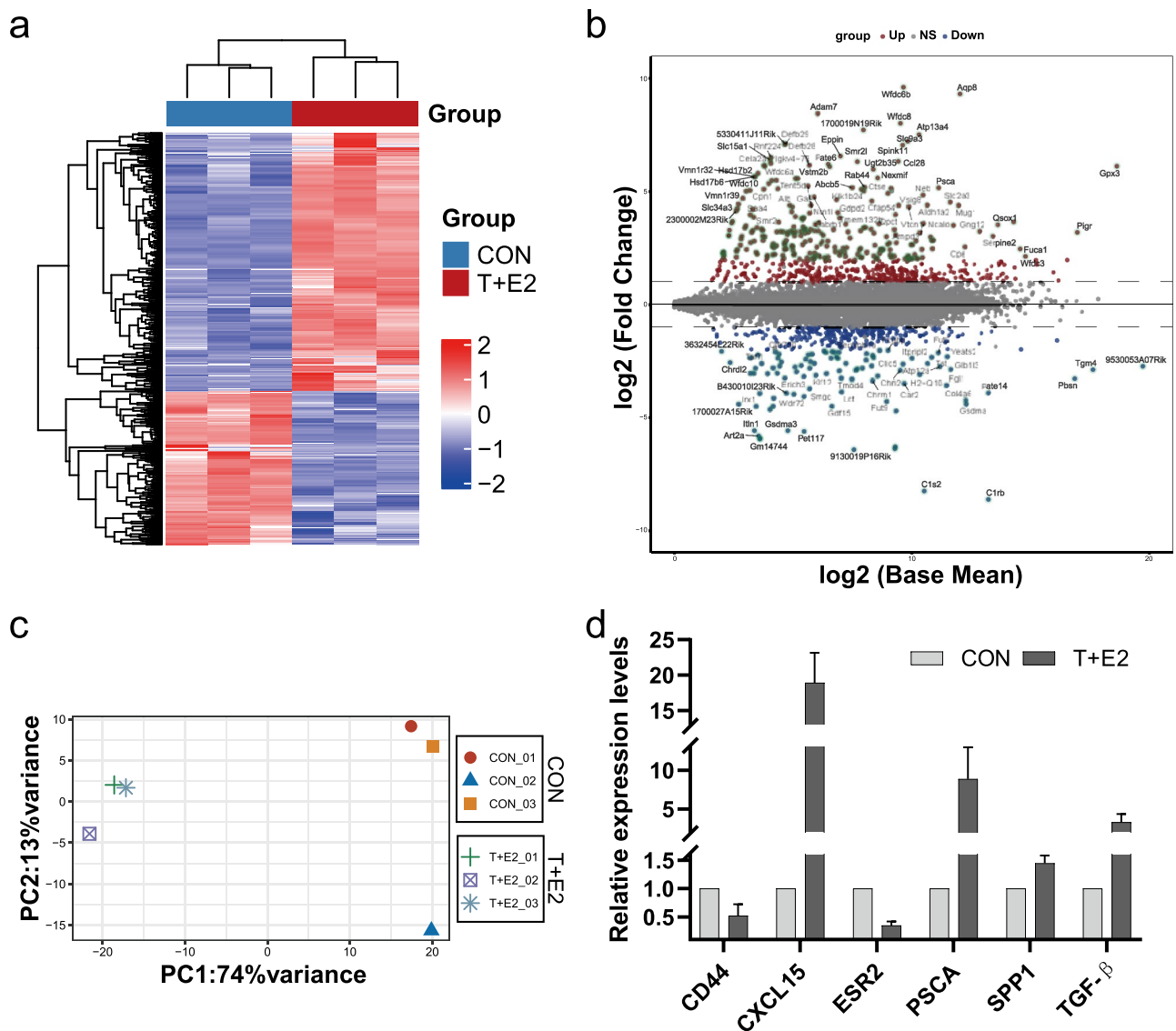
Fig. 3 Results of gene expression profile identification and validation of DEGs. **A** Heatmap diagram of DEGs between the CON and T + E2 groups. **B** Volcano plots showing DEGs (the horizontal dotted line marks log2-fold changes of 1 or -1). **C** PCA plot showing the clustering of the samples using all DEGs. **D** Six differentially expressed genes were validated by qRT−PCR

downregulated DEGs were mainly enriched in amino acid transport across the plasma membrane, metabolism of carbohydrates, and aldosterone synthesis and secretion. The up- and downregulated DEGs were mainly coenriched in mineral absorption, transport of small molecules, and amino acid metabolism (Fig. 4D, Table S8).

GSEA was performed for GO and KEGG analysis, and the results showed that the main terms were regulation of endopeptidases and peptidases and the complement and coagulation cascade pathways (Fig. S2–S3, Tables S9–10).

GSVA scores for GO items were high for positive regulation of cholesterol esterification (biological process (BP)), cellular response to insulin-like growth factor stimulus (BP), endoplasmic reticulum tubular network membrane (cellular component (CC)), phospholipid translocating ATPase complex (CC), and phosphate ion transmembrane transporter activity (molecular function (MF)) in the T + E2 group. In the CON group, mitochondrial translational elongation (BP), positive regulation of 3'UTR-mediated mRNA stabilization (BP), elastic fibre (CC), cell body fibre (CC), and leucine transmembrane transporter activity (MF) were scored high via GSVA (Fig. S4-A, B, C, Tables S11–13).

GSVA suggested that o-glycan biosynthesis, lysosome, complement and coagulation cascades, proteasome, and regulation of autophagy were scored high in the T + E2 group. In the CON group, valine, leucine, and isoleucine biosynthesis; Wnt signalling pathway; arginine and proline
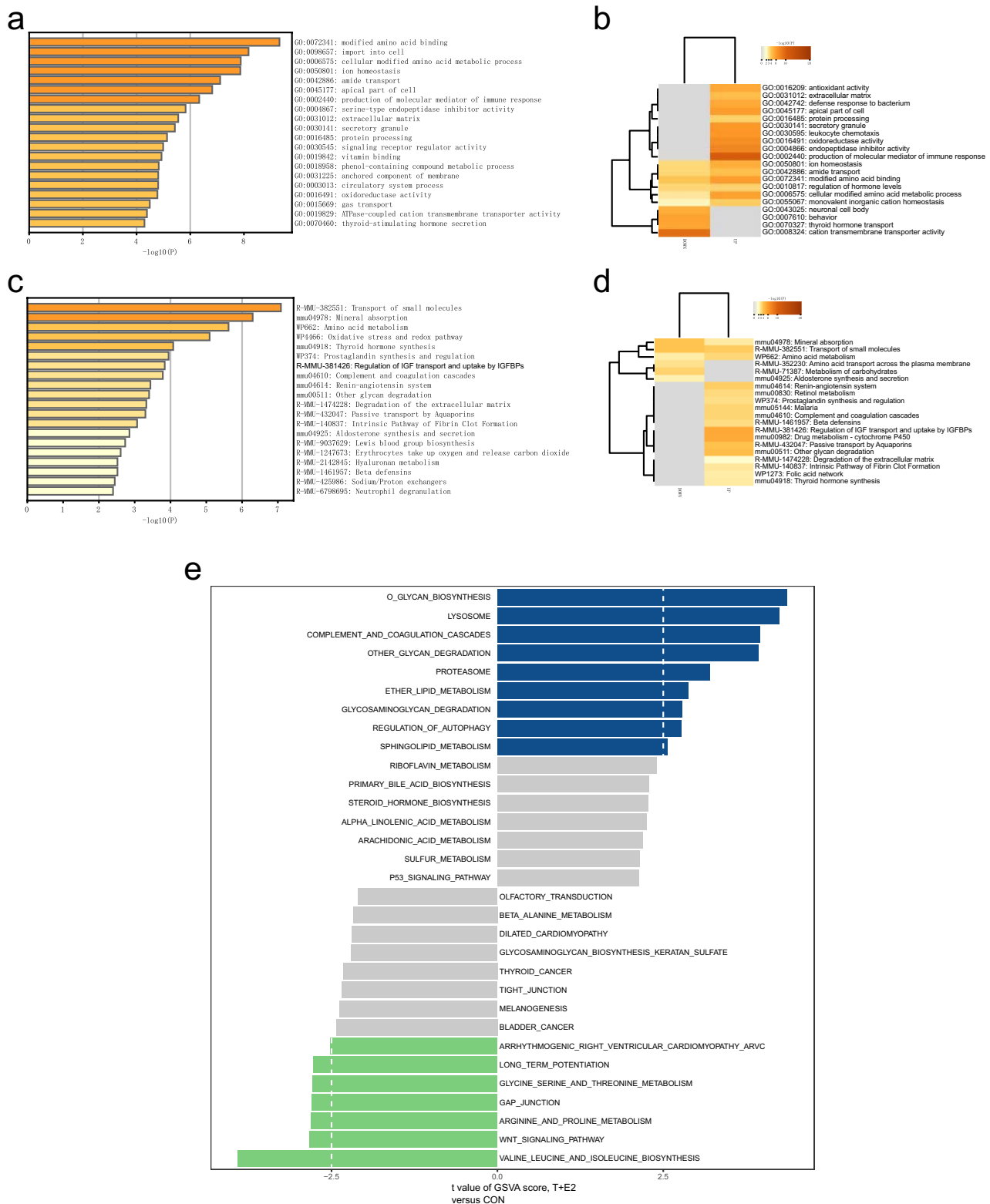
Fig. 4 Functional annotation and pathway enrichment analysis. **A** Bar graph of the top 20 enriched significant GO terms (Values represent -log10 p values); **B** GO enrichment analysis of upregulated and downregulated DEGs (Values represent -log10 p values); **C** bar graph shows the top 20 pathways (Values represent -log10 p values); **D** pathway enrichment analysis of upregulated and downregulated DEGs (Values represent -log10 P values); **E** bar plot of pathway score calculated by GSVA for the CON group and T+E2 group

metabolism; gap junctions; and glycine serine and threonine metabolism were highly scored (Fig. 4E, Table S14).

Construction of the PPI network and analysis of hub genes

The PPI networks constructed using Metascape, with 479 nodes and 1607 edges, were also divided into 16 significant modules based on different GO clusters (Fig. 5A, Table S15) and the genes in each module (Table S16). Module 5 was the most central module associated with antioxidant activity. Previous studies have demonstrated a close relationship between antioxidant activity and BPH [45]. All 13 genes from module 5 had the highest Macode score of the top 13, and the genes from module 5 were also used to generate the subsequent ceRNA network. Next, we used the five algorithms in Cytoscape's plugin "Cytohubba" to identify the top 30 genes for each and the key genes IGF1 and EPHA7 that were shared with the seed genes of the 16 important modules (Fig. 5B). In normal tissues obtained from the GTEx dataset, the levels of these 2 genes showed different correlations in different tissues (Fig. 5C), with a significant positive correlation between the levels of these 2 genes in prostate tissue ($P < 0.05$, Fig. 5D). We further examined the transcriptional data obtained from all BPH samples from 5 datasets (37 samples in total) from GEO and found a positive but nonsignificant correlation between the levels of 2 genes ($P > 0.05$, Fig. 5E, Table S17). A network of Igf1 and Epha7 interactions was generated using the genemania plugin in Cytoscape, and the 2 genes were found to be linked in various ways, including physical interactions, prediction, and coexpression.

Construction of the ceRNA network

To explore the molecular regulatory mechanisms of DEm-RNAs within the module of interest, lncRNA−miRNA-mRNA and circRNA-miRNA−mRNA regulatory networks were established. lncRNA-related ceRNA networks were generated, involving 199 molecules and 445 interactions, including those of 2 DEmRNAs, 172 predicted lncRNAs, and 25 predicted miRNAs (Fig. 6A, Tables S18–19). The other circRNA-associated ceRNA network, involving 300 genes and 608 interactions, included 2 DEmRNAs, 273 predicted circRNAs, and 25 predicted miRNAs (Fig. 6B, Tables S18, 20). ceRNA networks can enable an understanding of the regulatory relationships of these key genes and help discover more potential biological targets. For example, we focused on Hsd17b2, which could be regulated by miR-181a-5p, while lncRNA NEAT1 and circRNA Snx5 can regulate Hsd17b2 by competing for miRNA binding sites.

Immune cell infiltration

Using the CIBERSORT algorithm, we compared the infiltration levels of 25 subsets of immune cells in the prostate tissues between the two groups and found that all samples were infiltrated by multiple types of immune cells; for example, plasma cells and monocytes were the predominant immune cells in all samples, while eosinophils were less represented (Fig. 7), but there was no significant difference in the proportion of individual types of infiltrating immune cells when the two groups were compared ($P > 0.05$, Fig. S5).

Discussion

During adulthood, the prostate is the only solid organ that continues to grow continuously [46]. BPH has been found to be associated with quality-of-life (QoL) alterations and health problems in elderly men [47, 48]. In our study, mice treated with T + E2 showed not only the gross and pathological features of BPH but also features that have only observed in patients with progressive BPH, such as elongation and narrowing of the urethra in the prostate area, as well as bladder stones, which is consistent with secondary stones, and hydronephrosis and bladder wall thinning caused by BOO [49–53]. The elongation and narrowing of the urethra in the prostate might be a key factor in the development of BOO in BPH mice, and the elongation of the urethra at the junction with the bladder was particularly pronounced and might be related to the lack of fixation of the urethra in this area by tissues, such as smooth muscle, and the pull of the dilated bladder. The T + E2-induced mouse model of BPH has greater advantages than the rat model, as the characteristic alterations associated with BPH combined with BOO more closely resembled those in humans, while similar findings have not been reported for the steroid hormone-induced BPH rat model. In addition, the genetics of the mice was more fully explored, and the mature gene editing system in mice is more conducive to assessing the impact of changes in genetic information on biological functions [54, 55]. The protocol for inducing BPH mice with BOO in this study had the shortest known induction time, requiring only three subcutaneous implantations of slow-release pellets with a total induction time of 12 weeks, which leads to a lower risk of infection than traditional daily injections of sex hormones, facilitating the mass production of BPH-combined BOO mice. The T + E2-induced mouse model of BPH with BOO can provide a reliable research tool for the study of mechanisms related to BPH.

A proportion of patients with BPH who are treated clinically with medication eventually require surgery, accounting for approximately 10% [56], which reflects the limitations of current pharmacological treatment options. The
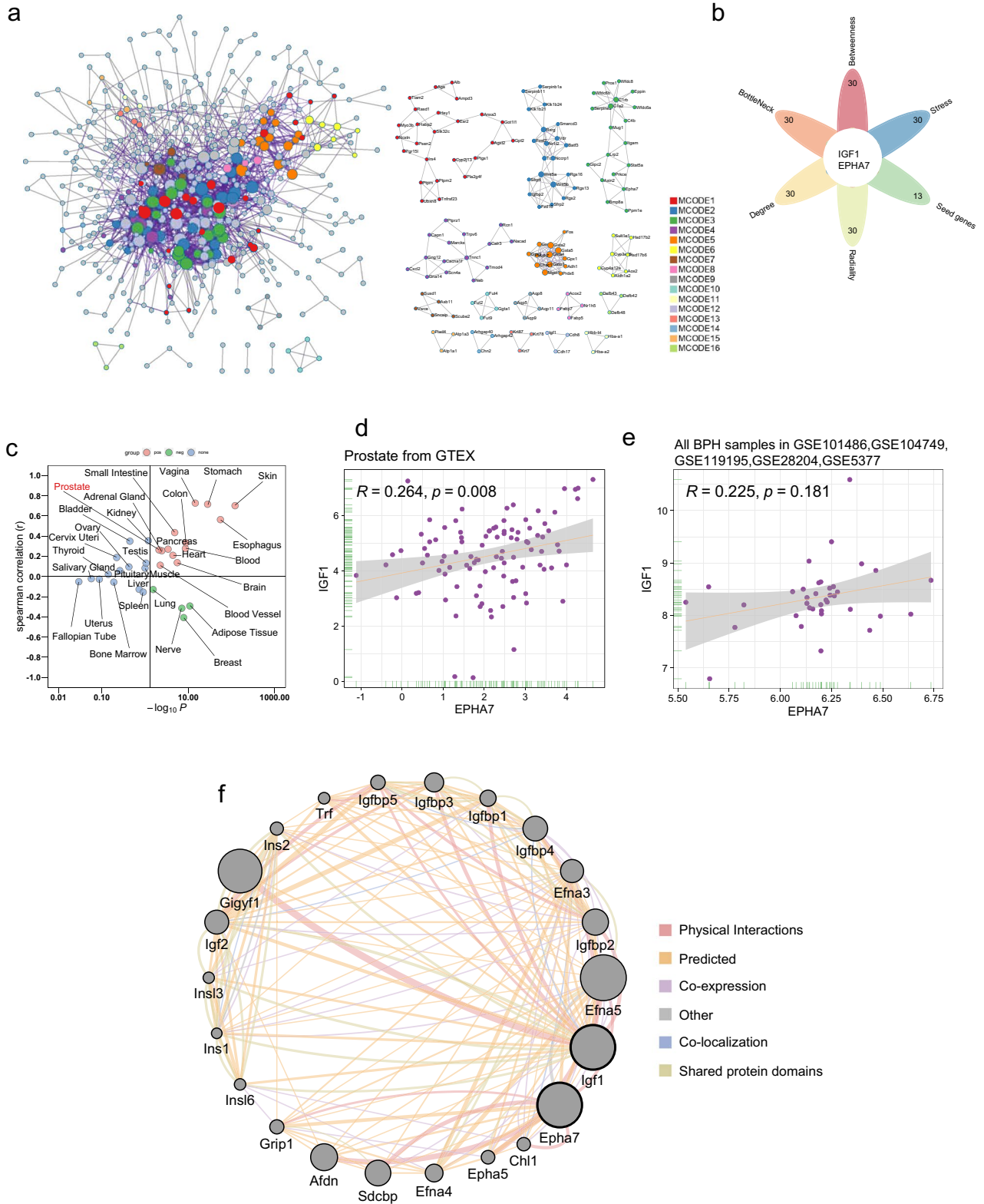
imbalance of androgen and oestrogen was considered to be one of the important pathogenic mechanisms underlying BPH, but there was no comprehensive and effective treatment for the imbalance [57], and the search for new therapeutic targets had become an urgent matter, but there was a lack of large-scale transcriptomic screening. This type

◄Fig. 5 PPI network of the DEGs was generated, and hub genes were analysed. **A** The PPI network and the 16 most significant MCODE components. **B** Flower plot shows the hub genes obtained by 6 algorithms. **C** A comparison of the expression levels of the hub genes in different normal tissues. **D** Scatterplot shows a positive correlation between IGF1 and EPHA7 expression levels in prostate tissue from the GTEx database ($P=0.008$); **E** Scatterplot shows a positive correlation between IGF1 and EPHA7 expression levels in the prostate of BPH patients from the GEO database ($P=0.181$); **F** GeneMANIA network: black circles represent inputs into GeneMANIA, and grey circles correspond to GeneMANIA proposed hubs

of screening is indispensable for an in-depth study of the molecular mechanisms involved in androgen- and oestrogen-induced BPH. By RNA-seq, 833 significantly differentially expressed genes were identified between the two groups. In the results of GO enrichment analysis, we found that upregulated DEGs were significantly enriched in redox processes, which was consistent with previous studies that the redox system was associated with the development of BPH [58]. The destruction of redox balance is easy to induce oxidative stress [59]. Oxidative stress is also considered to be one of the mechanisms that cause early pathological changes during prostate hyperplasia [60]. Oxidative stress can promote prostate hyperplasia by affecting the apoptosis pathway of prostate cells [61], inducing prostatitis [62, 63], and accelerating prostate proliferation [64] by activating the PI3K/Akt signalling pathway. Androgen can induce oxidative stress by increasing free radicals [65] and physiological amount of estrogen has antioxidant effect, but over-physiological amount of estrogen may induce oxidative stress by causing mitochondrial dysfunction [66]. However, the relationship between the ratio of estrogen/androgens and oxidative stress is still unknown, and further study is needed. Antioxidant stress may become a new therapeutic target for BPH; for example, previous studies have found that the lipid extract from the fruit of the Royal Palm of Cuba may treat prostatic hyperplasia through antioxidation [67]. GO terms enriched in the downregulated DEGs were associated with ion transport [68], whereas the upregulated DEGs were enriched in hormonal regulation, and previous studies had demonstrated the involvement of both androgens and oestrogens in the progression of BPH[23, 69]. In addition, the results of KEGG analysis suggested that the most significant pathway was small molecules, which had been shown in previous studies to influence the cell cycle, apoptosis and proliferation [70–72], whereas the upregulated DEGs were most significantly enriched in pathways associated with IGFs and IGFBPs, which have been previously shown to be associated with BPH [28, 73], and inhibition of IGF-1 secretion inhibited the proliferation of prostate epithelial cells [29]. Up- and downregulated DEGs were also predominantly coenriched in small molecule compound-related pathways, suggesting that this pathway might play an important role in

steroid hormone-induced BPH. It is well accepted that BPH is an androgen-dependent condition, as castrated individuals do not develop BPH [74]. In the prostate, 5 α-reductase converts testosterone into dihydrotestosterone, which in turn combines with the androgen receptor to promote prostatic hyperplasia. Steroid signalling through the androgen receptor is considered to be the key regulator of prostatic hyperplasia [75, 76]. In addition, oestrogen signalling plays an important role in the pathophysiology of prostatic hyperplasia, and oestrogen can regulate the proliferation of primary stromal cells and their expression of inflammatory factors during BPH [22, 31]. By increasing oestrogen to androgen ratios, upregulated AR expression may increase the sensitivity of the prostate to androgens, resulting in prostate hyperplasia [31]. To further explore steroid hormone-induced genomic differences in mice, we used GSEA and GSVA. GSEA results showed that terms enriched for GO and KEGG were mainly associated with the regulation of endopeptidases and peptidases and complement and coagulation. GSVA showed that enriched GO and KEGG terms were mainly associated with cellular responses to insulin-like growth factor stimulation and autophagy, which is consistent with previous studies that have shown that BPH is associated with insulin-like growth factor-mediated hormone imbalance [77] and impaired autophagy [78].

The PPI network generated in this study identified 16 important modules; for example, module 6 was mainly associated with oxidoreductase activity and the steroid metabolic process, and previous studies have shown that dysregulation of redox homeostasis was associated with the pathogenesis of prostate hyperplasia [58]. It is known that the development of BPH is dependent on steroid hormones [79]. The key genes IGF1 and EPHA7, important seed genes in the modules and hub genes in several algorithms, were also identified, and previous studies have shown that IGF1 is associated with the development of BPH [64, 80, 81]. Findings involving EPHA7 have not been reported in most studies of BPH, although one study found that EPHA7 expression was upregulated in BPH tissue or normal tissue compared to most PCa samples [82]. In correlation studies, we found different correlations between IGF1 and EPHA7 levels in different tissues, implying that they may have different interregulatory effects; the levels of these genes were positively correlated in organs of the digestive system, such as the small intestine, stomach, colon, pancreas, and oesophagus. However, they were negatively correlated in adipose tissue. In prostate tissue, IGF1 levels were positively correlated with EPHA7 levels. Then, we studied all BPH samples from 5 GEO datasets and found that the levels of the two genes were also positively correlated, but this result was not statistically significant, indicating the need for further validation with more samples. Further study of the interrelationship of the 2 genes revealed a high degree
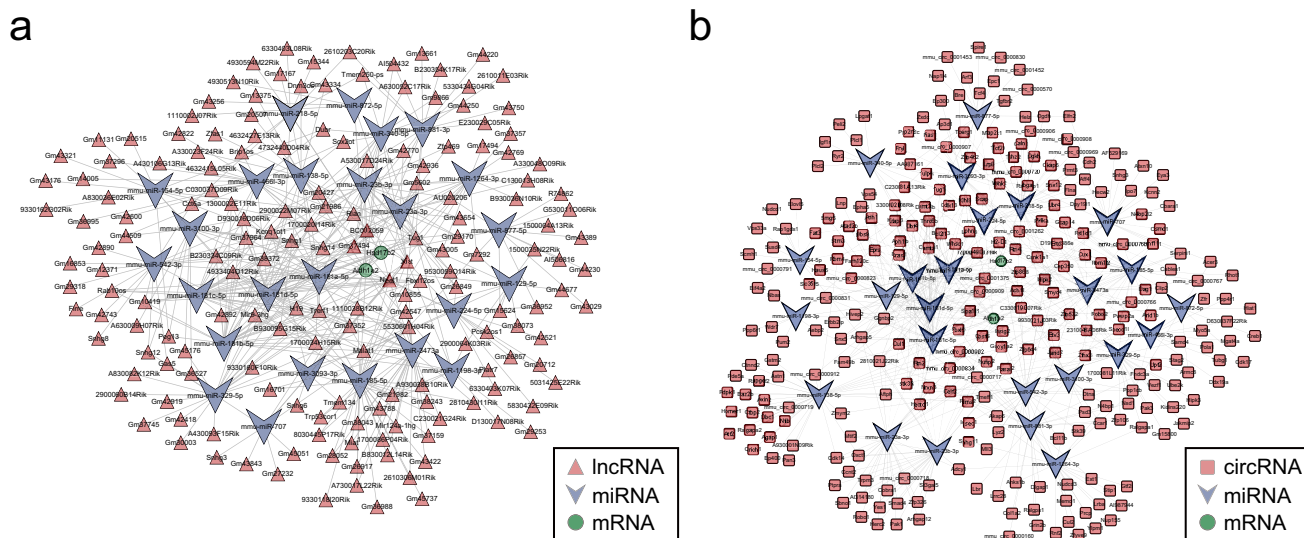
Fig. 6 Generation of ceRNA interaction network. **A** lncRNA−miRNA-mRNA ceRNA regulatory network; **B** circRNA-miRNA−mRNA ceRNA regulatory network
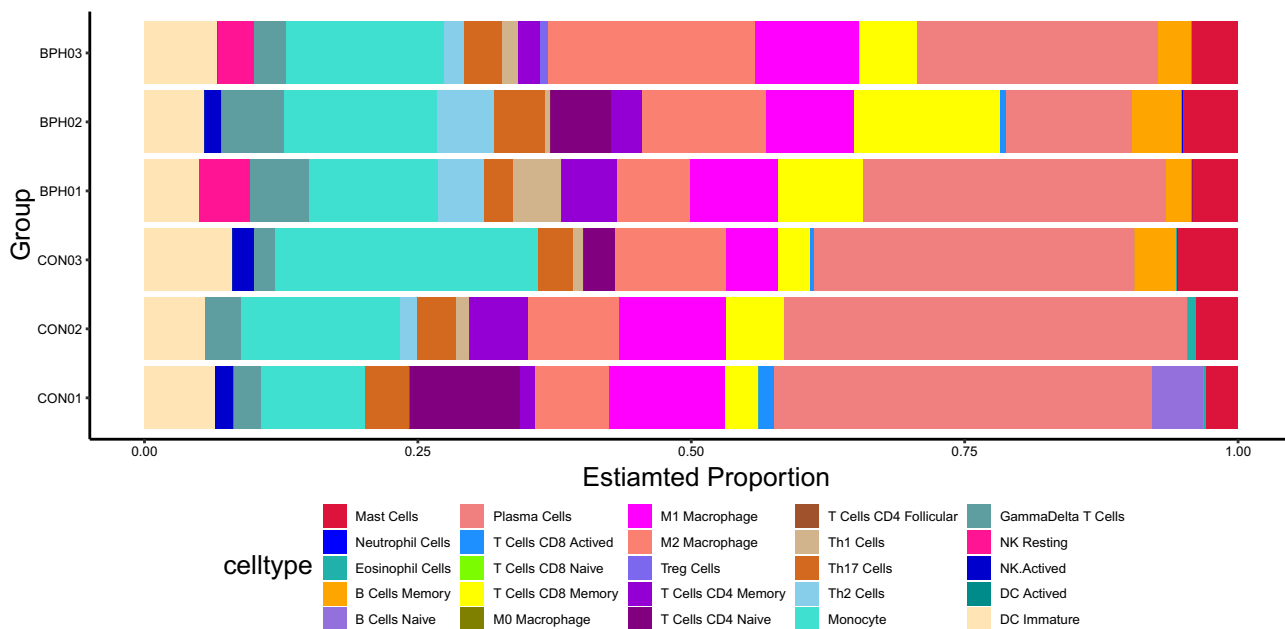

Fig. 7 Proportion of 25 immune cells in each sample from the CON and T+E2 groups

of interrelationship in a biological network with the 2 genes as the core; this interrelationship involved physical interactions, predicted, coexpression, colocalization, and shared protein domains in the network. We found many members of the Eph family and IGFBP family. As the largest family of tyrosine kinases, the Eph receptor has 14 members, and the binding site of its ligand (Ephrin) is located on the cell membrane [83]. In addition to modulating IGF bioactivity, IGFBP family members have independent biological actions

[84], and it was predicted by the network that IGF-1 might interact directly or indirectly with multiple IGFBP family and Eph family members. The network predicted that IGF-1 might interact directly or indirectly with several IGFBP and Eph family proteins, suggesting that these interactions might be related to the regulation of cell-to-cell crosstalk.

Based on the ceRNA hypothesis, lncRNAs (circR-NAs) might act as ceRNAs by acting as sponges for miR-NAs and thus indirectly regulate mRNA expression. The

expression of mRNAs in this network is regulated directly and indirectly by miRNAs and lncRNAs (circRNAs)[85]. Many noncoding RNAs in the generated ceRNA network might be involved in regulating these key genes, which in turn can influence the regulation of steroid hormone-induced BPH. For example, in the lncRNA-related ceRNA network, NEAT1 can regulate the expression of Hsd17b2, an mRNA related to steroid metabolism, via miR-181a-5p [86]. Steroid hormones were inactivated by HSD17B2, and their balance was regulated in a variety of tissues by this molecule [87]. The elevation in HSD17B2 levels may have been due to the supraphysiological dose of steroid hormone used in this experiment. In the circRNA-related reRNA network, circRNA Snx5 regulates Aldh1a2 (a retinoic acid synthase) via miR-129-5p, and elevated Aldh1a2 promotes retinoic acid synthesis, while retinoic acid (a vitamin A metabolite) also exhibits anti-inflammatory effects by preventing oxidative stress [87]; these findings suggest feedback regulation by mouse prostate tissue in response to intense oxidative stress. The above findings also suggest that steroid hormone-induced BPH in mice was regulated by a dynamic balance of oxidative stress and antioxidative stress.

In the immune infiltration analysis, we found no significant difference in the proportion of 25 immune cells after $T + E2$ treatment and similar levels of immune infiltration in both groups. Erin M. McAuley et al.[88] used $T + E2$ to treat mice and similarly found no effect on the distribution of immune cells in the prostate. Human BPH tissue contains infiltrating T lymphocytes, B lymphocytes and macrophages, which might drive fibromuscular growth during BPH by activating and coordinating the release of cell factors [89]. The time of our prostate sample collection might not have coincided with the time of immune infiltration, and more samples are needed to confirm the findings regarding immune infiltration in the model. The shift from experimental animals to clinical application needs to be continuously explored and validated.

Conclusion

In conclusion, we established a mouse model of BPH combined with BOO that is simple to manipulate and suitable for mass production. The model is associated with the specific alterations in histology and general pathology associated with BPH and provides a research platform for further studies of BPH. In this study, we also identified important genes and pathways involved in steroid-induced BPH and explored intermolecular regulatory relationships and immune features, and these results might provide new insights into the search for therapeutic targets for BPH.

Author contributions TXH: designed the study and wrote the manuscript. TXH, LZY, RJW, and YC: conducted animal experiments and pathological analyses. LZY: performed RNA extraction and qRT−PCR analysis. TXH and RJW: performed the data analysis. XSJ, SZL, and LGH: revised the manuscript. All authors have read and approved the published version of the manuscript.

Data availability Raw data files have been deposited to the Gene Expression Omnibus Database (www.ncbi.nlm.nih.gov/geo/), and accession number is GSE218403.

Declarations

References

1. Lim KB (2017) Epidemiology of clinical benign prostatic hyperplasia. Asian J Urol 4:148–151. https://doi.org/10.1016/j.ajur.2017.06.004
2. Chughtai B, Forde JC, Thomas DD, Laor L, Hossack T, Woo HH, Te AE, Kaplan SA (2016) Benign prostatic hyperplasia. Nat Rev Dis Primers 2:16031. https://doi.org/10.1038/nrdp.2016.31
3. Lee CL, Kuo HC (2017) Pathophysiology of benign prostate enlargement and lower urinary tract symptoms: current concepts. Ci Ji Yi Xue Za Zhi 29:79–83. https://doi.org/10.4103/tcmj.tcmj_20_17
4. Foo KT (2019) What is a disease? What is the disease clinical benign prostatic hyperplasia (BPH)? World J Urol 37:1293–1296. https://doi.org/10.1007/s00345-019-02691-0
5. Murray CJ, Vos T, Lozano R, Naghavi M, Flaxman AD, Michaud C, Ezzati M, Shibuya K, Salomon JA, Abdalla S, Aboyans V,

Abraham J, Ackerman I, Aggarwal R, Ahn SY, Ali MK, Alvarado M, Anderson HR, Anderson LM, Andrews KG, Atkinson C, Baddour LM, Bahalim AN, Barker-Collo S, Barrero LH, Bartels DH, Basáñez MG, Baxter A, Bell ML, Benjamin EJ, Bennett D, Bernabé E, Bhalla K, Bhandari B, Bikbov B, Bin Abdulhak A, Birbeck G, Black JA, Blencowe H, Blore JD, Blyth F, Bolliger I, Bonaventure A, Boufous S, Bourne R, Boussinesq M, Braithwaite T, Brayne C, Bridgett L, Brooker S, Brooks P, Brugha TS, Bryan-Hancock C, Bucello C, Buchbinder R, Buckle G, Budke CM, Burch M, Burney P, Burstein R, Calabria B, Campbell B, Canter CE, Carabin H, Carapetis J, Carmona L, Cella C, Charlson F, Chen H, Cheng AT, Chou D, Chugh SS, Coffeng LE, Colan SD, Colquhoun S, Colson KE, Condon J, Connor MD, Cooper LT, Corriere M, Cortinovis M, de Vaccaro KC, Couser W, Cowie BC, Criqui MH, Cross M, Dabhadkar KC, Dahiya M, Dahodwala N, Damsere-Derry J, Danaei G, Davis A, De Leo D, Degenhardt L, Dellavalle R, Delossantos A, Denenberg J, Derrett S, Des Jarlais DC, Dharmaratne SD, Dherani M, Diaz-Torne C, Dolk H, Dorsey ER, Driscoll T, Duber H, Ebel B, Edmond K, Elbaz A, Ali SE, Erskine H, Erwin PJ, Espindola P, Ewoigbokhan SE, Farzadfar F, Feigin V, Felson DT, Ferrari A, Ferri CP, Fèvre EM, Finucane MM, Flaxman S, Flood L, Foreman K, Forouzanfar MH, Fowkes FG, Fransen M, Freeman MK, Gabbe BJ, Gabriel SE, Gakidou E, Ganatra HA, Garcia B, Gaspari F, Gillum RF, Gmel G, Gonzalez-Medina D, Gosselin R, Grainger R, Grant B, Groeger J, Guillemin F, Gunnell D, Gupta R, Haagsma J, Hagan H, Halasa YA, Hall W, Haring D, Haro JM, Harrison JE, Havmoeller R, Hay RJ, Higashi H, Hill C, Hoen B, Hoffman H, Hotez PJ, Hoy D, Huang JJ, Ibeanusi SE, Jacobsen KH, James SL, Jarvis D, Jasrasaria R, Jayaraman S, Johns N, Jonas JB, Karthikeyan G, Kassebaum N, Kawakami N, Keren A, Khoo JP, King CH, Knowlton LM, Kobusingye O, Koranteng A, Krishnamurthi R, Laden F, Lalloo R, Laslett LL, Lathlean T, Leasher JL, Lee YY, Leigh J, Levinson D, Lim SS, Limb E, Lin JK, Lipnick M, Lipshultz SE, Liu W, Loane M, Ohno SL, Lyons R, Mabweijano J, MacIntyre MF, Malekzadeh R, Mallinger L, Manivannan S, Marcenes W, March L, Margolis DJ, Marks GB, Marks R, Matsumori A, Matzopoulos R, Mayosi BM, McAnulty JH, McDermott MM, McGill N, McGrath J, Medina-Mora ME, Meltzer M, Mensah GA, Merriman TR, Meyer AC, Miglioli V, Miller M, Miller TR, Mitchell PB, Mock C, Mocumbi AO, Moffitt TE, Mokdad AA, Monasta L, Montico M, Moradi-Lakeh M, Moran A, Morawska L, Mori R, Murdoch ME, Mwaniki MK, Naidoo K, Nair MN, Naldi L, Narayan KM, Nelson PK, Nelson RG, Nevitt MC, Newton CR, Nolte S, Norman P, Norman R, O'Donnell M, O'Hanlon S, Olives C, Omer SB, Ortblad K, Osborne R, Ozgediz D, Page A, Pahari B, Pandian JD, Rivero AP, Patten SB, Pearce N, Padilla RP, Perez-Ruiz F, Perico N, Pesudovs K, Phillips D, Phillips MR, Pierce K, Pion S, Polanczyk GV, Polinder S, Pope CA 3rd, Popova S, Porrini E, Pourmalek F, Prince M, Pullan RL, Ramaiah KD, Ranganathan D, Razavi H, Regan M, Rehm JT, Rein DB, Remuzzi G, Richardson K, Rivara FP, Roberts T, Robinson C, De Leòn FR, Ronfani L, Room R, Rosenfeld LC, Rushton L, Sacco RL, Saha S, Sampson U, Sanchez-Riera L, Sanman E, Schwebel DC, Scott JG, Segui-Gomez M, Shahraz S, Shepard DS, Shin H, Shivakoti R, Singh D, Singh GM, Singh JA, Singleton J, Sleet DA, Sliwa K, Smith E, Smith JL, Stapelberg NJ, Steer A, Steiner T, Stolk WA, Stovner LJ, Sudfeld C, Syed S, Tamburlini G, Tavakkoli M, Taylor HR, Taylor JA, Taylor WJ, Thomas B, Thomson WM, Thurston GD, Tleyjeh IM, Tonelli M, Towbin JA, Truelsen T, Tsilimbaris MK, Ubeda C, Undurraga EA, van der Werf MJ, van Os J, Vavilala MS, Venketasubramanian N, Wang M, Wang W, Watt K, Weatherall DJ, Weinstock MA, Weintraub R, Weisskopf MG, Weissman MM, White RA, Whiteford H, Wiebe N, Wiersma ST, Wilkinson JD, Williams HC, Williams SR, Witt E, Wolfe F, Woolf AD, Wulf S, Yeh PH, Zaidi AK, Zheng ZJ, Zonies D, Lopez AD, AlMazroa MA, Memish ZA (2012) Disability-adjusted life years (DALYs) for 291 diseases and injuries in 21 regions, 1990-2010: a systematic analysis for the global burden of disease study 2010. Lancet 380:2197–223. https://doi.org/10.1016/s0140-6736(12)61689-4

6. La Vignera S, Aversa A, Cannarella R, Condorelli RA, Duca Y, Russo GI, Calogero AE (2021) Pharmacological treatment of lower urinary tract symptoms in benign prostatic hyperplasia: consequences on sexual function and possible endocrine effects. Expert Opin Pharmacother 22:179–189. https://doi.org/10.1080/14656566.2020.1817382

7. Yang BY, Jiang CY, Dai CY, Zhao RZ, Wang XJ, Zhu YP, Qian YX, Yin FL, Fu XY, Jing YF, Han BM, Xia SJ, Ruan Y (2019) 5-ARI induces autophagy of prostate epithelial cells through suppressing IGF-1 expression in prostate fibroblasts. Cell Prolif 52:e12590. https://doi.org/10.1111/cpr.12590

8. Strebel RT, Kaplan SA (2021) The state of TURP through a historical lens. World J Urol 39:2255–2262. https://doi.org/10.1007/s00345-021-03607-7

9. Cai T, Cui Y, Yu S, Li Q, Zhou Z, Gao Z (2020) Comparison of serenoa repens with tamsulosin in the treatment of benign prostatic hyperplasia: a systematic review and meta-analysis. Am J Mens Health 14:1557988320905407. https://doi.org/10.1177/1557988320905407

10. Nachawati D, Patel JB (2022) Alpha Blockers. StatPearls Publishing LLC, Treasure Island (FL)

11. Yang MH, Huang YH, Hsieh TY, Wang SC, Chen WJ, Lee TH, Chen SL (2020) Pyuria and post-operation urinary tract infection after diode laser vaporesection of the prostate. Surg Infect (Larchmt) 21:255–261. https://doi.org/10.1089/sur.2019.117

12. Chen LK, Lai YW, Chiu LP, Chen SS (2021) Significant relationship between parameters measured by transrectal color Doppler ultrasound and sexual dysfunction in patients with BPH 12 months after TURP. BMC Urol 21:9. https://doi.org/10.1186/s12894-020-00776-2

13. Ambrosini GL, de Klerk NH, Mackerras D, Leavy J, Fritschi L (2008) Dietary patterns and surgically treated benign prostatic hyperplasia: a case control study in Western Australia. BJU Int 101:853–860. https://doi.org/10.1111/j.1464-410X.2007.07345.x

14. Kim BS, Ko YH, Song PH, Kim TH, Kim KH, Kim BH (2019) Prostatic urethral length as a predictive factor for surgical treatment of benign prostatic hyperplasia: a prospective, multiinstitutional study. Prostate Int 7:30–34. https://doi.org/10.1016/j.prnil.2018.06.002

15. Jahan N, Chowdhury A, Li T, Xu K, Wei F, Wang S (2021) Neferine improves oxidative stress and apoptosis in benign prostate hyperplasia via Nrf2-ARE pathway. Redox Rep 26:1–9. https://doi.org/10.1080/13510002.2021.1871814

16. Vickman RE, Franco OE, Moline DC, Vander Griend DJ, Thumbikat P, Hayward SW (2020) The role of the androgen receptor in prostate development and benign prostatic hyperplasia: A review. Asian J Urol 7:191–202. https://doi.org/10.1016/j.ajur.2019.10.003

17. Li Y, Ge C, Franceschi RT (2021) Role of Runx2 in prostate development and stem cell function. Prostate 81:231–241. https://doi.org/10.1002/pros.24099

18. Azadeh F, Gharib FZ, Hosseini SM (2022) Effects of *glycyrrhiza glabra* (licorice) root extract on the hormones, serum biochemicals, and hematological parameters in dogs with benign prostatic hyperplasia. Evid Based Complement Alternat Med 2022:8962889. https://doi.org/10.1155/2022/8962889

19. Csikós E, Horváth A, Ács K, Papp N, Balázs VL, Dolenc MS, Kenda M, Kočevar Glavač N, Nagy M, Protti M, Mercolini L, Horváth G, Farkas Á, On Behalf Of The O (2021) Treatment of benign prostatic hyperplasia by natural drugs. Molecules. https://doi.org/10.3390/molecules26237141

20. Aversa A, Duca Y, Condorelli RA, Calogero AE, La Vignera S (2019) Androgen deficiency and phosphodiesterase type 5 expression changes in aging male: therapeutic implications. Front Endocrinol (Lausanne) 10:225. https://doi.org/10.3389/fendo.2019.00225

21. Hyde Z, Flicker L, Hankey GJ, Almeida OP, McCaul KA, Chubb SA, Yeap BB (2010) Prevalence of sexual activity and associated factors in men aged 75 to 95 years: a cohort study. Ann Intern Med 153:693–702. https://doi.org/10.7326/0003-4819-153-11-201012070-00002

22. Chen B, Cao D, Chen Z, Huang Y, Lin T, Ai J, Liu L, Wei Q (2020) Estrogen regulates the proliferation and inflammatory expression of primary stromal cell in benign prostatic hyperplasia. Transl Androl Urol 9:322–331. https://doi.org/10.21037/tau.2020.02.08

23. Yang Y, Sheng J, Hu S, Cui Y, Xiao J, Yu W, Peng J, Han W, He Q, Fan Y, Niu Y, Lin J, Tian Y, Chang C, Yeh S, Jin J (2022) Estrogen and G protein-coupled estrogen receptor accelerate the progression of benign prostatic hyperplasia by inducing prostatic fibrosis. Cell Death Dis 13:533. https://doi.org/10.1038/s41419-022-04979-3

24. Nicholson TM, Ricke EA, Marker PC, Miano JM, Mayer RD, Timms BG, vom Saal FS, Wood RW, Ricke WA (2012) Testosterone and 17β-estradiol induce glandular prostatic growth, bladder outlet obstruction, and voiding dysfunction in male mice. Endocrinology 153:5556–5565. https://doi.org/10.1210/en.2012-1522

25. Lucia MS, Lambert JR (2008) Growth factors in benign prostatic hyperplasia: basic science implications. Curr Urol Rep 9:272–278. https://doi.org/10.1007/s11934-008-0048-6

26. Boguslawska J, Kryst P, Poletajew S, Piekielko-Witkowska A (2019) TGF-β and microRNA interplay in genitourinary cancers. Cells. https://doi.org/10.3390/cells8121619

27. Frantzi M, Latosinska A, Belczacka I, Mischak H (2019) Urinary proteomic biomarkers in oncology: ready for implementation? Expert Rev Proteomics 16:49–63. https://doi.org/10.1080/14789450.2018.1547193

28. Calogero AE, Burgio G, Condorelli RA, Cannarella R, La Vignera S (2019) Epidemiology and risk factors of lower urinary tract symptoms/benign prostatic hyperplasia and erectile dysfunction. Aging Male 22:12–19. https://doi.org/10.1080/13685538.2018.1434772

29. Yuan YF, Zhu WX, Liu T, He JQ, Zhou Q, Zhou X, Zhang X, Yang J (2020) Cyclopamine functions as a suppressor of benign prostatic hyperplasia by inhibiting epithelial and stromal cell proliferation via suppression of the Hedgehog signaling pathway. Int J Mol Med 46:311–319. https://doi.org/10.3892/ijmm.2020.4569

30. Eyman D, Damodarasamy M, Plymate SR, Reed MJ (2009) CCL5 secreted by senescent aged fibroblasts induces proliferation of prostate epithelial cells and expression of genes that modulate angiogenesis. J Cell Physiol 220:376–381. https://doi.org/10.1002/jcp.21776

31. Wu S, Huang D, Su X, Yan H, Ma A, Li L, Wu J, Sun Z (2020) The prostaglandin synthases, COX-2 and L-PGDS, mediate prostate hyperplasia induced by low-dose bisphenol A. Sci Rep 10:13108. https://doi.org/10.1038/s41598-020-69809-y

32. Xin R, Gao Y, Gao Y, Wang R, Kadash-Edmondson KE, Liu B, Wang Y, Lin L, Xing Y (2021) isoCirc catalogs full-length circular RNA isoforms in human transcriptomes. Nat Commun 12:266. https://doi.org/10.1038/s41467-020-20459-8

33. Mendelevich A, Vinogradova S, Gupta S, Mironov AA, Sunyaev SR, Gimelbrant AA (2021) Replicate sequencing libraries are important for quantification of allelic imbalance. Nat Commun 12:3370. https://doi.org/10.1038/s41467-021-23544-8

34. Derbis M, Kul E, Niewiadomska D, Sekrecki M, Piasecka A, Taylor K, Hukema RK, Stork O, Sobczak K (2021) Short antisense oligonucleotides alleviate the pleiotropic toxicity of RNA harboring expanded CGG repeats. Nat Commun 12:1265. https://doi.org/10.1038/s41467-021-21021-w

35. Hermida LC, Gertz EM, Ruppin E (2022) Predicting cancer prognosis and drug response from the tumor microbiome. Nat Commun 13:2896. https://doi.org/10.1038/s41467-022-30512-3

36. Wilks C, Zheng SC, Chen FY, Charles R, Solomon B, Ling JP, Imada EL, Zhang D, Joseph L, Leek JT, Jaffe AE, Nellore A, Collado-Torres L, Hansen KD, Langmead B (2021) recount3: summaries and queries for large-scale RNA-seq expression and splicing. Genome Biol 22:323. https://doi.org/10.1186/s13059-021-02533-6

37. Rioux G, Ridha Z, Simard M, Turgeon F, Guérin SL, Pouliot R (2020) Transcriptome Profiling Analyses in Psoriasis: A Dynamic Contribution of Keratinocytes to the Pathogenesis. Genes (Basel). https://doi.org/10.3390/genes11101155

38. Zhang H, Tian Y, Yang B, An LY, Xia SJ, Luo GH (2021) A novel mouse model simulating transurethral laser vaporization prostatectomy. Asian J Androl. https://doi.org/10.4103/aja.aja_59_21

39. Zhou Y, Zhou B, Pache L, Chang M, Khodabakhshi AH, Tanaseichuk O, Benner C, Chanda SK (2019) Metascape provides a biologist-oriented resource for the analysis of systems-level datasets. Nat Commun 10:1523. https://doi.org/10.1038/s41467-019-09234-6

40. Subramanian A, Tamayo P, Mootha VK, Mukherjee S, Ebert BL, Gillette MA, Paulovich A, Pomeroy SL, Golub TR, Lander ES, Mesirov JP (2005) Gene set enrichment analysis: a knowledge-based approach for interpreting genome-wide expression profiles. Proc Natl Acad Sci U S A 102:15545–15550. https://doi.org/10.1073/pnas.0506580102

41. Rahman M, MacNeil SM, Jenkins DF, Shrestha G, Wyatt SR, McQuerry JA, Piccolo SR, Heiser LM, Gray JW, Johnson WE, Bild AH (2017) Activity of distinct growth factor receptor network components in breast tumors uncovers two biologically relevant subtypes. Genome Med 9:40. https://doi.org/10.1186/s13073-017-0429-x

42. Thomson DW, Dinger ME (2016) Endogenous microRNA sponges: evidence and controversy. Nat Rev Genet 17:272–283. https://doi.org/10.1038/nrg.2016.20

43. Newman AM, Liu CL, Green MR, Gentles AJ, Feng W, Xu Y, Hoang CD, Diehn M, Alizadeh AA (2015) Robust enumeration of cell subsets from tissue expression profiles. Nat Methods 12:453–457. https://doi.org/10.1038/nmeth.3337

44. Chen Z, Huang A, Sun J, Jiang T, Qin FX, Wu A (2017) Inference of immune cell composition on the expression profiles of mouse tissue. Sci Rep 7:40508. https://doi.org/10.1038/srep40508

45. Kim KS, Yang HY, Chang SC, Kim YM, Lee KY, Lee BM, Kim HS (2018) Potential repositioning of GV1001 as a therapeutic agent for testosterone-induced benign prostatic hyperplasia. Int J Mol Med 42:2260–2268. https://doi.org/10.3892/ijmm.2018.3759

46. Loeb S, Kettermann A, Carter HB, Ferrucci L, Metter EJ, Walsh PC (2009) Prostate volume changes over time: results from the baltimore longitudinal study of aging. J Urol 182:1458–1462. https://doi.org/10.1016/j.juro.2009.06.047

47. Loffroy R, Guillen K, Salet E, Marcelin C, Comby PO, Midulla M, Grenier N, Chevallier O, Petitpierre F (2021) Prostate artery embolization using n-butyl cyanoacrylate glue for urinary tract symptoms due to benign prostatic hyperplasia: a valid alternative to microparticles? J Clin Med. https://doi.org/10.3390/jcm10143161

48. Gudmundsson J, Sigurdsson JK, Stefansdottir L, Agnarsson BA, Isaksson HJ, Stefansson OA, Gudjonsson SA, Gudbjartsson DF, Masson G, Frigge ML, Stacey SN, Sulem P, Halldorsson GH, Tragante V, Holm H, Eyjolfsson GI, Sigurdardottir O, Olafsson I, Jonsson T, Jonsson E, Barkardottir RB, Hilmarsson R, Asselbergs

FW, Geirsson G, Thorsteinsdottir U, Rafnar T, Thorleifsson G, Stefansson K (2018) Genome-wide associations for benign prostatic hyperplasia reveal a genetic correlation with serum levels of PSA. Nat Commun 9:4568. https://doi.org/10.1038/s41467-018-06920-9

49. Kim EH, Larson JA, Andriole GL (2016) Management of benign prostatic hyperplasia. Annu Rev Med 67:137–151. https://doi.org/10.1146/annurev-med-063014-123902

50. Kim NH, Jegal J, Kim YN, Heo JD, Rho JR, Yang MH, Jeong EJ (2020) The effects of aronia melanocarpa extract on testosterone-induced benign prostatic hyperplasia in rats, and quantitative analysis of major constituents depending on extract conditions. Nutrients. https://doi.org/10.3390/nu12061575

51. Moore A, Butcher MJ, Köhler TS (2015) Testosterone replacement therapy on the natural history of prostate disease. Curr Urol Rep 16:51. https://doi.org/10.1007/s11934-015-0526-6

52. Long JD, Smith SR (2021) Prostatic urethral lift for the treatment of lower urinary tract symptoms in men with benign prostatic hyperplasia: a cochrane review summary. Int J Nurs Stud. 115:103492. https://doi.org/10.1016/j.ijnurstu.2019.103492

53. Garimella PS, Fink HA, Macdonald R, Wilt TJ (2009) Naftopidil for the treatment of lower urinary tract symptoms compatible with benign prostatic hyperplasia. Cochrane Database Syst Rev. https://doi.org/10.1002/14651858.CD007360.pub2

54. Zhou M, Liu Y, Ma C (2021) Distinct nuclear architecture of photoreceptors and light-induced behaviors in different strains of mice. Transl Vis Sci Technol 10:37. https://doi.org/10.1167/tvst.10.2.37

55. Cao Y, Vergnes L, Wang YC, Pan C, Chella Krishnan K, Moore TM, Rosa-Garrido M, Kimball TH, Zhou Z, Charugundla S, Rau CD, Seldin MM, Wang J, Wang Y, Vondriska TM, Reue K, Lusis AJ (2022) Sex differences in heart mitochondria regulate diastolic dysfunction. Nat Commun 13:3850. https://doi.org/10.1038/s41467-022-31544-5

56. Cindolo L, Pirozzi L, Sountoulides P, Fanizza C, Romero M, Castellan P, Antonelli A, Simeone C, Tubaro A, de Nunzio C, Schips L (2015) Patient's adherence on pharmacological therapy for benign prostatic hyperplasia (BPH)-associated lower urinary tract symptoms (LUTS) is different: is combination therapy better than monotherapy? BMC Urol 15:96. https://doi.org/10.1186/s12894-015-0090-x

57. Nicholson TM, Moses MA, Uchtmann KS, Keil KP, Bjorling DE, Vezina CM, Wood RW, Ricke WA (2015) Estrogen receptor-α is a key mediator and therapeutic target for bladder complications of benign prostatic hyperplasia. J Urol 193:722–729. https://doi.org/10.1016/j.juro.2014.08.093

58. Sampson N, Koziel R, Zenzmaier C, Bubendorf L, Plas E, Jansen-Dürr P, Berger P (2011) ROS signaling by NOX4 drives fibroblast-to-myofibroblast differentiation in the diseased prostatic stroma. Mol Endocrinol 25:503–515. https://doi.org/10.1210/me.2010-0340

59. Zhang J, Morris-Natschke SL, Ma D, Shang XF, Yang CJ, Liu YQ, Lee KH (2021) Biologically active indolizidine alkaloids. Med Res Rev 41:928–960. https://doi.org/10.1002/med.21747

60. White EZ, Pennant NM, Carter JR, Hawsawi O, Odero-Marah V, Hinton CV (2020) Serum deprivation initiates adaptation and survival to oxidative stress in prostate cancer cells. Sci Rep 10:12505. https://doi.org/10.1038/s41598-020-68668-x

61. Sakata S, Hayashi S, Fujishiro T, Kawakita K, Kanzaki N, Hashimoto S, Iwasa K, Chinzei N, Kihara S, Haneda M, Ueha T, Nishiyama T, Kuroda R, Kurosaka M (2015) Oxidative stress-induced apoptosis and matrix loss of chondrocytes is inhibited by eicosapentaenoic acid. J Orthop Res 33:359–365. https://doi.org/10.1002/jor.22767

62. Šutulović N, Grubač Ž, Šuvakov S, Jerotić D, Puškaš N, Macut D, Rašić-Marković A, Simić T, Stanojlović O, Hrnčić D (2021) Experimental chronic prostatitis/chronic pelvic pain syndrome increases anxiety-like behavior: the role of brain oxidative stress, serum corticosterone, and hippocampal parvalbumin-positive interneurons. Oxid Med Cell Longev 2021:6687493. https://doi.org/10.1155/2021/6687493

63. Jang YJ, Jung HY, Myeong JY, Song KH, Kwon J, Kim D, Park JI (2023) Effects of alginate oligosaccharide on testosterone-induced benign prostatic hyperplasia in orchiectomized rats. Nutrients. https://doi.org/10.3390/nu15030682

64. Omar HA, Tolba MF (2018) Caffeic acid phenethyl ester guards against benign prostate hypertrophy in rats: Role of IGF-1R/protein kinase-B (Akt)/β-catenin signaling. IUBMB Life 70:519–528. https://doi.org/10.1002/iub.1743

65. Cunningham RL, Giuffrida A, Roberts JL (2009) Androgens induce dopaminergic neurotoxicity via caspase-3-dependent activation of protein kinase Cdelta. Endocrinology 150:5539–5548. https://doi.org/10.1210/en.2009-0640

66. Huang JC, Duan CC, Jin S, Sheng CB, Wang YS, Yue ZP, Guo B (2022) HB-EGF induces mitochondrial dysfunction via estrogen hypersecretion in granulosa cells dependent on cAMP-PKA-JNK/ERK-Ca(2+)-FOXO1 pathway. Int J Biol Sci 18:2047–2059. https://doi.org/10.7150/ijbs.69343

67. Perez Y, Molina V, Mas R, Menendez R, Gonzalez RM, Oyarzabal A, Jimenez S (2008) Ex vivo antioxidant effects of D-004, a lipid extract from Roystonea regia fruits, on rat prostate tissue. Asian J Androl 10:659–666. https://doi.org/10.1111/j.1745-7262.2008.00385.x

68. Wan SS, Zhang L, Zhang XZ (2019) An ATP-regulated ion transport nanosystem for homeostatic perturbation therapy and sensitizing photodynamic therapy by autophagy inhibition of tumors. ACS Cent Sci 5:327–340. https://doi.org/10.1021/acscentsci.8b00822

69. Xu Z, Ge Y, Jiang K, Xu L, Zhu J, Zhou C, Zhou L, Jia R (2021) Effects of shRNA-mediated silencing of PDE5A3 on intracellular cGMP and free Ca(2+) levels and human prostate smooth muscle cell proliferation from benign prostatic hyperplasia. Exp Ther Med 21:322. https://doi.org/10.3892/etm.2021.9753

70. Hu X, Hao F, Li X, Xun Z, Gao Y, Ren B, Cang M, Liang H, Liu D (2021) Generation of VEGF knock-in Cashmere goat via the CRISPR/Cas9 system. Int J Biol Sci 17:1026–1040. https://doi.org/10.7150/ijbs.55559

71. Santagata S, Ieranò C, Trotta AM, Capiluongo A, Auletta F, Guardascione G, Scala S (2021) CXCR4 and CXCR7 Signaling Pathways: A Focus on the Cross-Talk Between Cancer Cells and Tumor Microenvironment. Front Oncol. 11:591386. https://doi.org/10.3389/fonc.2021.591386

72. Jenkins T, Gouge J (2021) Nrf2 in cancer, detoxifying enzymes and cell death programs. Antioxidants (Basel). https://doi.org/10.3390/antiox10071030

73. Wang Z, Olumi AF (2011) Diabetes, growth hormone-insulin-like growth factor pathways and association to benign prostatic hyperplasia. Differentiation 82:261–271. https://doi.org/10.1016/j.diff.2011.04.004

74. Jacobsen SJ (2007) Risk factors for benign prostatic hyperplasia. Curr Urol Rep 8:281–288. https://doi.org/10.1007/s11934-007-0074-9

75. Leiblich A, Hellberg J, Sekar A, Gandy C, Mendes CC, Redhai S, Mason J, Wainwright M, Marie P, Goberdhan DCI, Hamdy FC, Wilson C (2019) Mating induces switch from hormone-dependent to hormone-independent steroid receptor-mediated growth in Drosophila secondary cells. PLoS Biol 17:3000145. https://doi.org/10.1371/journal.pbio.3000145

76. Lao K, Xun G, Gou X, Xiang H (2019) Design, synthesis, and biological evaluation of novel androst-17β-amide structurally related compounds as dual 5α-reductase inhibitors and androgen receptor antagonists. J Enzyme Inhib Med Chem 34:1597–1606. https://doi.org/10.1080/14756366.2019.1654469

77. Chen KC, Sung SY, Lin YT, Hsieh CL, Shen KH, Peng CC, Peng RY (2015) Benign prostatic hyperplasia complicated with T1DM can be alleviated by treadmill exercise-evidences revealed by the rat model. BMC Urol 15:113. https://doi.org/10.1186/s12894-015-0104-8

78. Den C, Giglio S, Baldassarri V, Cirombella R, Mallel G, Nacchia A, Tubaro A, Vecchione A (2021) Impairment of autophagy may represent the molecular mechanism behind the relationship between obesity and inflammation in patients with BPH and LUTS. Minerva Urol Nephrol 73:631–637. https://doi.org/10.23736/s2724-6051.20.03992-2

79. Xu D, Wu Y, Shen H, Qian S, Qi J (2020) High serum concentration of estradiol may be a risk factor of prostate enlargement in aging male in China. Aging Male 23:1–6. https://doi.org/10.1080/13685538.2018.1481027

80. Kumar S, Yadav RN, Gupta P, Gaspar BL, Kakkar N, Verma A, Parthan G, Bhansali A, Mukherjee KK, Korbonits M, Dutta P (2015) Prostatic hyperplasia in acromegaly, a myth or reality: a case-control study. Eur J Endocrinol 172:97–106. https://doi.org/10.1530/eje-14-0698

81. Wang Z, Olumi AF (2018) Metformin: an antiproliferative agent and methylation regulator in treating prostatic disease? Am J Physiol Renal Physiol 314:F407-f411. https://doi.org/10.1152/ajprenal.00443.2017

82. Li S, Wu Z, Ma P, Xu Y, Chen Y, Wang H, He P, Kang Z, Yin L, Zhao Y, Zhang X, Xu X, Ma X, Guan M (2017) Ligand-dependent EphA7 signaling inhibits prostate tumor growth and progression. Cell Death Dis 8:e3122. https://doi.org/10.1038/cddis.2017.507

83. Wen Z, Liu Q, Wu J, Xu B, Wang J, Liang L, Guo Y, Peng M, Zhao Y, Liao Q (2019) Fibroblast activation protein α-positive pancreatic stellate cells promote the migration and invasion of pancreatic cancer by CXCL1-mediated Akt phosphorylation. Ann Transl Med 7:532. https://doi.org/10.21037/atm.2019.09.164

84. Ren J, Anversa P (2015) The insulin-like growth factor I system: physiological and pathophysiological implication in cardiovascular diseases associated with metabolic syndrome. Biochem Pharmacol 93:409–417. https://doi.org/10.1016/j.bcp.2014.12.006

85. Shi F, Xu H, Liu C, Tan C, Ren J, Ye X, Feng H, Liu Z (2021) Whole-transcriptome sequencing reveals a vernalization-related ceRNA regulatory network in chinese cabbage (Brassica campestris L. ssp. pekinensis). BMC Genomics 22:819. https://doi.org/10.1186/s12864-021-08110-2

86. Lai ZZ, Yang HL, Shi JW, Shen HH, Wang Y, Chang KK, Zhang T, Ye JF, Sun JS, Qiu XM, Li MQ (2021) Protopanaxadiol improves endometriosis associated infertility and miscarriage in sex hormones receptors-dependent and independent manners. Int J Biol Sci 17:1878–1894. https://doi.org/10.7150/ijbs.58657

87. Drzewiecka H, Jarmołowska-Jurczyszyn D, Kluk A, Gałęcki B, Dyszkiewicz W, Jagodziński PP (2020) Altered expression of 17-β-hydroxysteroid dehydrogenase type 2 and its prognostic significance in non-small cell lung cancer. Int J Oncol 56:1352–1372. https://doi.org/10.3892/ijo.2020.5014

88. McAuley EM, Mustafi D, Simons BW, Valek R, Zamora M, Markiewicz E, Lamperis S, Williams A, Roman BB, Vezina C, Karczmar G, Oto A, Vander Griend DJ (2017) Magnetic resonance imaging and molecular characterization of a hormone-mediated murine model of prostate enlargement and bladder outlet obstruction. Am J Pathol 187:2378–2387. https://doi.org/10.1016/j.ajpath.2017.07.014

89. De Nunzio C, Presicce F, Tubaro A (2016) Inflammatory mediators in the development and progression of benign prostatic hyperplasia. Nat Rev Urol 13:613–626. https://doi.org/10.1038/nrurol.2016.168